Research Article

TANKYRASE INHIBITION REGULATES CORPUS LUTEUM DEVELOPMENT AND LUTEAL FUNCTION IN GONADOTROPIN-TREATED RATS†

Running title: Wnt/β-catenin in corpus luteum development and function.

Accialini Paula[1], Irusta Griselda[1], Bechis Andres[1,2], Bas Diana[1], Parborell Fernanda[1], Abramovich Dalhia[1], Tesone Marta[1, 2]

[1]Instituto de Biología y Medicina Experimental (IBYME-CONICET), Buenos Aires, Argentina.

[2] Departamento de Quıímica Biológica, Facultad de Ciencias Exactas y Naturales, Universidad de Buenos Aires, Buenos Aires, Argentina.

Abbreviations:

FSH, Follicle-stimulating hormone; LH, Luteinizing hormone; cytochrome P450scc, cytochrome P450 side-chain cleavage (also known as CYP11A1); STAR, Steroidogenic acute regulatory protein; VEGF, Vascular endothelial growth factor.

Supported by Universidad de Buenos Aires (UBA 20020090300061), CONICET (PIP 1223), ANPCYT (PICT 2010-0248) and Rene Baron Foundation, Argentina.

Correspondence: Marta Tesone, Instituto de Biologia y Medicina Experimental, Vuelta de Obligado 2490, Buenos Aires, 1428, Argentina. FAX: 54 11 4786 2564; e-mail: martatesone.uba@gmail.com

†This article has been accepted for publication and undergone full peer review but has not been through the copyediting, typesetting, pagination and proofreading process, which may lead to differences between this version and the Version of Record. Please cite this article as doi: [10.1002/jmv.22853]

Received 26 January 2017; Revised 19 May 2017; Accepted 11 June 2017

Journal of Medical Virology

DOI 10.1002/jmv.22853

ABSTRACT

Tankyrases are physiological regulators of Axin, a protein involved in several cellular processes, including Wnt signaling. Here, we investigated the effect of a specific Tankyrase inhibitor (XAV939) in follicular-luteal dynamics, and its possible relationship with ovarian vascular development. Studies were designed to analyze the effect of intrabursa administration of XAV939 in gonadotropin-treated prepubertal rats. In particular, we examined follicle and corpus luteum development, steroidogenesis, angiogenic markers, and apoptotic parameters. We found that in vivo inhibition of Wnt signaling impaired corpus luteum development, with a decrease in the number of corpora lutea balanced by a high number of cysts; decreased circulating progesterone levels, likely due to a decrease in Steroidogenic acute regulatory protein content in the corpus luteum; and increased pro-apoptotic parameters. In addition, Extracellular signal-regulated kinase phosphorylation, Vascular endothelium growth factor 120 content, and endothelial cell area were diminished in corpora lutea of inhibitor-treated ovaries. Thus Wnt/β-catenin signaling appears to participate in the regulation of corpus luteum development and luteal cell function.

Keywords: Tankyrase inhibitor, Wnt/β-catenin, luteinization, steroidogenesis, progesterone

INTRODUCTION

The gonadotropins Follicle-stimulating hormone (FSH) and Luteinizing hormone (LH) are the main endocrine factors that regulate ovarian follicle and corpus luteum development, with several paracrine and autocrine growth factors acting as local regulators (Chun, Billig et al. 1994, Tilly and Tilly 1995, Abramovich, Parborell et al. 2006, Pascuali, Scotti et al. 2015). During luteolysis, FSH and LH induce a complex pattern of gene expression in ovarian cells that is regulated by the coordinated input from different signaling cascades, such as the cyclic Adenosine monophosphate/Protein kinase A, Phosphoinositide 3-kinase /AKT, and Extracellular signal-regulated kinase 1/2 pathways (Hunzicker-Dunn and Maizels 2006). Members of the BCL2 family have also been described as apoptotic regulatory factors in luteal cells (Korsmeyer 1992).

Luteolysis is accompanied by changes to steroid production, vasculature, and cell survival that are each controlled by specific regulatory factors. Ovarian steroid biosynthesis is regulated by the enzymatic conversion of cholesterol to pregnenolone, which is catalyzed by the cytochrome P450scc enzyme (P450 side-chain cleavage, encoded by the gene *CYP11A1*). Cholesterol is actively delivered to the inner mitochondrial membrane by Steroidogenic acute regulatory protein (StAR) (reviewed in (Stocco, Telleria et al. 2007). Members of the Wnt (Wingless-type mouse mammary tumor virus integration site) family were recently described as intraovarian regulators of follicle growth and corpus luteum development (reviewed by Hernandez Gifford 2015). Wnt signaling pathway is a highly conserved system composed of secreted glycoproteins with local action that regulate key processes related to homeostasis, development, proliferation, and cell death. Canonical

pathway activation involves binding of Wnt ligands to the seven-transmembrane receptor Frizzled. This interaction results in the accumulation of hypo-phosphorylated β-catenin, which translocates to the nucleus, where it regulates transcription factor activity. When the system is not stimulated, β-catenin levels are low due to the action of a β-catenin destruction complex composed of Adenomatous polyposis coli (APC), Axin, and Glycogen synthase kinase 3 β (GSK-3β). Axin is the limiting factor that regulates the efficiency of the β-catenin destruction complex (Boyer, Goff et al. 2010).

Various Wnt components are expressed in the postnatal ovary and some of them are differentially expressed during follicular development, suggesting a potential role for this system in follicle formation, ovulation, and luteinization (Vainio, Heikkila et al. 1999); (Tomizuka, Horikoshi et al. 2008). Wnt components are expressed in granulosa, theca, and cumulus cells and in the corpora lutea of human and rodent ovaries (Boyer, Goff et al. 2010), and the abundance of Wnt members in growing follicles increases after human Chorionic gonadotropin administration in rodents (Hsieh, Mulders et al. 2003). The role of WNT regulating the function of FSH on cattle follicular cells has also been described (Gupta, Folger et al. 2014, Abedini, Zamberlam et al. 2015). The importance of Wnt signaling in the ovary is demonstrated by the phenotype associated with *Wnt4* ovarian conditional-knockout mice, which exhibit a 75% reduction in antral follicles that is probably due to increased follicular atresia (Boyer, Lapointe et al. 2010). Luteal progesterone synthesis is also decreased in granulosa cell-specific *Wnt4*-knockout mice, which is mediated by a decrease in the abundance of transcripts encoding STAR, cytochrome P450scc, and cytochrome P450 aromatase (encoded by the Cyp19a1 gene)

(Boyer, Goff et al. 2010). In contrast, overexpression of *Wnt4* in mouse granulosa cells increased the abundance of these transcripts (Boyer, Goff et al. 2010).

VEGF-A plays a pivotal role in ovarian angiogenesis, in particular through the regulation of follicular and CL development induced by LH (Christenson and Stouffer 1997, Martinez-Chequer, Stouffer et al. 2003, Abramovich, Parborell et al. 2006). The canonical Wnt/β-catenin pathway is implicated in angiogenesis, vascular remodeling and differentiation in various species and organ systems (Reis and Liebner 2013).

Little is known about the precise role of the Wnt/β-catenin signaling in the follicular-luteal dynamics, and its possible relationship to ovarian vascular development. We hypothesized that Wnt signaling contributes to regulation of gonadotropin-dependent luteinization. We tested this by assessing the effect of intrabursa administration of a specific Tankyrase inhibitor (XAV939) on gonadotropin-treated prepubertal rats. Tankyrases are enzymes that add poly-ADP-ribose to substrates (PARsylate) (Hsiao and Smith 2008) present in various tissues, including the ovary (Smith, Giriat et al. 1998; Kaminker, Kim et al. 2001; Lyons, Deane et al. 2001; Cook, Dynek et al. 2002), XAV939 is a small molecule that inhibits Tankyrase 1 and Tankyrase 2, leading to the stabilization of Axin, thereby fostering β-catenin degradation – and consequently blocking all downstream canonical Wnt signaling. In the present work we examined the effect of Tankyrase inhibition on follicle and corpus luteum development, steroidogenesis, angiogenesis, and apoptosis.

RESULTS

In vivo effect of XAV939 treatment on luteal β-catenin levels

β-catenin abundance was measured in corpora lutea protein extracts Western blot following XAV939 intrabursa administration to assess the potency of this small molecule. No significant changes were observed at 48 h after administration of 1 µg (control, 0.28±0.008 versus XAV939, 0.28±0.08 [n=4 each]; *P*=0.93). Conversely, β-catenin abundance significantly decreased after treatment with 5 µg (control, 0.87±0.01 [n=3] versus XAV939, 0.63±0.06 [n=4]; P<0.05) and 10 µg (control, 0.87±0.01 [n=3] versus XAV939, 0.72±0.01 [n=4]; *P*<0.01). Both 5 µg and 10 µg doses produced the same changes in luteal β-catenin abundance and serum progesterone concentration, so the 5 µg dose was chosen for subsequence experiments.

β-catenin abundance decreased both 24 and 48 hours after administration of 5 µg of XAV939 (Figure 1). The level of nuclear β-catenin, which is responsible for transcriptional regulation, also decreased following 5 µg XAV939 administration, as measured by Western blot (control, 1.7±0.04 versus XAV939, 1.4±0.05 [n=4 each]; *P*<0.01).

In vivo effect of Wnt/β-catenin pathway inhibition on follicular development

The acute effect of XAV939 administration on follicular development was tracked (Table 1). No significant differences were found in any stage of follicles analyzed, whereas the percentage of corpora lutea significantly decreased in ovaries injected with XAV939 compared to the control group (*P*<0.05). Interestingly, treatment with the Tankyrase

inhibitor produced cystic structures not present in the control animals (P<0.001) (Figure 2a).

Wnt/β-catenin signaling was also inhibited using ICG-001, which specifically down-regulates the expression of a subset of β-catenin/T-cell factor-responsive genes. Consistent with the cystic phenotype following XAV939 administration, ICG-001 produced ovarian cysts 48 hours after administration of 5 μg (control, 0% versus ICG-001, 1.22±0.33%) (Figure 2b). A decrease in the percentage of corpora lutea was also observed (control, 43.5±4.5% [n=6] versus ICG-001, 25.9±1.5% [n=5]; P<0.05). Similar results were observed after administration of 10 μg ICG-001 (data not shown).

Effect of Tankyrase inhibition on serum progesterone levels and steroidogenic regulators in the corpus luteum

Blood samples and ovaries were collected 48 hours after intrabursa XAV939 injection to evaluate the concentration of circulating progesterone and related steroidogenic factors in the ovary. Serum progesterone concentration significantly decreased after XAV939 administration (XAV939, 30.0±3.1 ng/ml versus control, 45.1±5.5 ng/ml [n=8 each]; P<0.05) (Figure 3a). The corpus luteal abundance of StAR, cytochrome P450scc, and 3β-hydroxysteroid dehydrogenase (3β-HSD) was also determined by Western blot. A significant decrease in StAR protein abundance was observed after XAV939 treatment (Figure 3b), whereas the levels of cytochrome P450scc (Figure 3c) and 3β-HSD (Figure 3d) did not change in comparison to the control group.

Involvement of ovarian Tankyrase inhibition in luteal proliferation and apoptotic parameters

The abundance of Proliferating cell nuclear antigen (PCNA), expressed in G1 and S phases of the cell cycle (Maga and Hubscher 2003), was measured by Western blot to examine if Wnt/β-catenin signaling is involved in corpus luteal cell proliferation. PCNA protein levels significantly decreased 48 hours after XAV939 treatment in comparison to the control group (Figure 4a). Furthermore, immunohistochemical staining revealed the presence of PCNA in small cells of corpora lutea, corresponding to small luteal cells and/or other corpus luteum components, such as endothelial cells (Figure 4b).

Protein levels of pro-apoptotic BAX and $BCLX_S$ and anti-apoptotic $BCLX_L$ were also measured by Western blot. Treatment with XAV939 significantly increased $BCLX_S$ protein abundance (Figure 5a) while significantly decreasing $BCLX_L$ content (Figure 5c). Consequently, the pro-apoptotic $BCLX_S$:$BCLX_L$ ratio significantly increased in the corpora lutea of treated ovaries compared to the control ovaries (Figure 5d). Even though XAV939 treatment did not affect BAX protein content (Figure 5b), the pro-apoptotic BAX:$BCLX_L$ ratio was significantly increased in the corpora lutea of treated ovaries (Figure 5e).

In vivo effect of Tankyrase inhibition on ERK and AKT signaling pathways in corpora lutea

To determine whether the Wnt/β-catenin pathway regulated by Tankyrases is involved in the phosphorylation of ERK and AKT, we performed a Western blot of the total and phosphorylated forms of ERK and AKT (pERK and pAKT respectively) in corpora lutea protein extracts 24 and 48 hours after XAV939 administration. No differences were found

48 hours after XAV939 treatment (data not shown). After 24 hours, ERK phosphorylation was significantly decreased in the inhibitor-treated samples compared to controls (Figure 6a); conversely, AKT phosphorylation was unchanged (Figure 6b).

Effect of Tankyrase inhibition on angiogenic factors and vascular development

VEGF isoforms and endothelial cell area were analyzed to determine if the Wnt/β-catenin pathway is involved in angiogenesis regulation. The abundance of VEGF isoforms 164 and 120 were measured 48 hours after XAV939 administration. No differences were observed between groups (data not shown). Moreover, VEGF luteal levels were evaluated 24 hours after the surgery. While VEGF164 (Figure 7a) content was no different between groups, VEGF120 was significantly lower in treated ovaries compared to the control group (Figure 7b). Endothelial cells were stained with *Bandeiraea simplicifolia* 1 lectin, and the positively stained area was quantified in the corpora lutea of treated and control ovarian sections 48 hours after XAV939 treatment. The XAV939-treated group showed a significant decrease in the percentage of endothelial cell area compared to the control group (Figure 8). The antibody used for VEGF quantification detects both angiogenic and anti-angiogenic isoforms. The decrease observed in VEGF120 is accompanied by a decrease in the percentage of endothelial cell area (lectin staining), suggesting that in the balance between angiogenic/antiangiogenic isoforms, the angiogenic VEGF120a isoform would be affected by our treatment.

DISCUSSION

The present study was designed to determine how administration of a specific Tankyrase inhibitor would modulate Wnt/β-catenin signaling in gonadotropin-treated prepubertal rats. We demonstrated, for the first time, that in vivo inhibition of Wnt signaling impairs corpus luteum development, primarily by decreasing the number of corpora lutea and the formation of ovarian cysts; lowering STAR abundance, which decreased circulating progesterone levels; promoting apoptosis; and decreasing cell proliferation as well as ERK phosphorylation. In addition, VEGF120 content and endothelial cell area were also diminished in the corpora lutea of inhibitor-treated ovaries. Together, these observations suggest that downstream Wnt/β-catenin signaling participates in the regulation of corpus luteum development and luteal cell function.

The crucial role of LH during luteinization is well demonstrated; however, autocrine and paracrine factors are able to modulate LH action locally (Stocco, Telleria et al. 2007). Wnt signaling regulates many developmental processes, including differentiation, proliferation, and apoptosis (Logan and Nusse 2004) – each of which is dynamically involved with corpus luteum function. Wnt ligands and Frizzled G receptor are expressed in developing follicles and corpora lutea of rats, mice, humans, and cattle (Hsieh, Johnson et al. 2002; Hernandez Gifford 2015). WNT2 and WNT4 in particular were extensively studied in the postnatal ovary, primarily by genetic manipulation of specific components of the Wnt pathway (Hsieh, Johnson et al. 2002; Hernandez Gifford 2015). Here, we used the small-molecule inhibitor XAV939 to decrease total and nuclear β-catenin content, thus affecting the activity of most canonical Wnt signaling in the ovary.

XAV939 enhances β-catenin degradation by stabilizing Axin, the concentration-limiting component of its destruction complex (Huang, Mishina et al. 2009). Although Axin plays a crucial role in Wnt signaling, it is also participates in Transforming growth factor beta, p53, and Mitogen-activated protein kinase signaling (Liu, Rui et al. 2006; Guo, Ramirez et al. 2008; Li, Lin et al. 2009). We therefore performed key experiments with the Wnt/β-catenin inhibitor ICG-001, which has a different mechanism of action than XAV939 (Grigson, Ozerova et al. 2015), to address phenotype specificity.

Blocking Wnt signaling in gonadotropin-treated rat ovaries, using either XAV939 or ICG-001, did not affect follicle stages, whereas ovulation and luteinization were impaired. Indeed, the number of corpora lutea significantly decreased while a significant number of cystic structures formed. These cysts were large, unruptured follicles containing an oocyte and an attenuated granulosa cell layer surrounded by luteal cells, and clearly differed from ovarian cyst generated by an excess of androgens in a polycystic ovarian syndrome rat model (Abramovich, Irusta et al. 2012). This novel follicle phenotype points to the involvement of Wnt/β-catenin signaling in the LH-induced ovulatory cascade. These results also correlate with decreased circulating progesterone levels, which may be related to the reduction in STAR protein abundance in corpora lutea. StAR regulates the delivery of cholesterol to mitochondria, and is considered the rate-limiting of progesterone biosynthesis in steroidogenic tissues (Stocco and Clark 1996). Conversely, no differences in abundance were observed for factors involved in later steroidogenic steps, such as cytochrome P450scc, an enzyme that catalyzes the conversion of cholesterol to pregnenolone (Lieberman, Greenfield et al. 1984); (Waterman and Simpson 1985), or 3β-HSD, the enzyme involved in progesterone synthesis from pregnenolone (Peng, Arensburg

et al. 2002). These findings are in agreement with a previous report in bovine luteal cells linking LH-stimulated steroidogenesis, STAR expression, and reductions in β-catenin through overexpression of GSK-3β (Roy, McDonald et al. 2009).

In addition to the poor ovulation phenotype, we observed that ovarian inhibition of Wnt signaling in gonadotropin-treated rats modified downstream signaling dependent on β-catenin. Although some reports implicate Wnt signaling as a modulator of AKT activity (Boyer, Goff et al. 2010), we did not observe any changes to AKT phosphorylation in our experimental model at the time points assessed. Conversely, XAV939-induced Wnt inhibition decreased ERK phosphorylation, suggesting some degree of crosstalk between ERK and canonical Wnt pathways in corpus luteal cells. Whether or not such signaling is related to the increased pro-apoptotic $BCLX_S$:$BCLX_L$ and pro-apoptotic BAX:$BCLX_L$ ratios, which enhanced apoptosis of the corpus luteal cells, remains to be determined. Experiments are in progress in our laboratory to further understand the molecular mechanism by which Wnt contributes to corpus luteum development.

The formation of new blood vessels in the ovary is essential to supply the nutrients and hormones that promote follicular growth and corpus luteum formation (Redmer and Reynolds 1996, Tamanini and De Ambrogi 2004). Much evidence supports a role for the canonical and non-canonical Wnt pathways in vascular development, primarily by controlling the production of angiogenic factors (Reis and Liebner 2013). VEGF is the main initiator of angiogenesis, and acts by stimulating endothelial cell proliferation. Establishing a mature vascular network, however, requires the coordinated action of many additional factors, including Angiopoietins 1 and 2, which act via the tyrosine kinase receptor, Tie-2 (Maisonpierre, Suri et al. 1997), and Platelet-derived growth factor B

(Carmeliet and Jain 2011, Scotti, Parborell et al. 2014). Together, these pro-angiogenic factors recruit peri-vascular cells that mature and stabilize newly formed capillaries (Suri, Jones et al. 1996, Maisonpierre, Suri et al. 1997). However, to our knowledge, no studies regarding Wnt signaling and CL angiogenesis have been performed. In the corpus luteum, we observed a significant decrease in the percentage of endothelial cell area and in the abundance of VEGF120 after administration of XAV939. The abundance of proliferation marker PCNA, particularly in small luteal cells and to other components of the corpus luteum, also decreased after inhibitor treatment. Indeed, cell proliferation during luteolysis does not cease: although the division of granulosa cells stops, mitosis occurs in the theca layer and fibroblasts and endothelial cells continue to divide (Peluso, Luciano et al. 1995). Growth of the corpora lutea in rodents primarily results from an increase in the size of large luteal cells (hypertrophy), while the number of small luteal cells and endothelial cells expands (Bachelot and Binart 2005). Ultimately, the vascular changes associated with XAV939 treatment may have contributed to the observed impairment in the luteinization process. For example, different VEGF isoforms are known to promote specific functions in certain vascular beds (Maes, Carmeliet et al. 2002), and are differentially expressed during corpus luteum progression (Tesone, Stouffer et al. 2005). Clearly, further studies are needed to elucidate the precise contribution of Wnt signaling to endothelial cell growth and blood vessel stabilization during corpus luteum development.

In summary, the results of the present study provide the first evidence that Wnt/β-catenin system regulates the luteinization process in gonadotropin–treated rats. We demonstrated that the Wnt canonical pathway is involved in ovulation process and luteal progesterone production through the regulation of StAR levels. In addition, Wnt inhibition

increases pro:anti-apoptotic CL protein ratio, decreases CL ERK phosphorylation and regulates the ovarian vascular development (Figure 9).

MATERIALS AND METHODS

Superovulation and in vivo ovarian inhibition of Tankyrase 1 and 2

Immature female Sprague-Dawley rats (21 to 23 days old) were housed at room temperature, with a 12:12h light-dark photoperiod in an air-conditioned environment and *ad libitum* access to food and water. Rats were subcutaneously injected with equine chorionic gonadotropin (eCG) (25 IU/rat), and 48 hours later with human Chorionic Gonadotropin (hCG) (10 IU/rat). The day of hCG administration, the rats were anesthetized with ketamine HCl (80 mg/kg) (Holliday-Scott, Buenos Aires, Argentina) and xylazine (4 mg/kg) (Konig Laboratories, Buenos Aires, Argentina). The ovaries were exteriorized through an incision made in the dorsal lumbar region for intrabursal injection. This administration route was chosen to limit diffusion of the inhibitor to the contralateral ovary, which may occur due to the low molecular weight and the hydrophobic characteristic of the inhibitors used; however, a minimal systemic effect cannot be ruled out. A pituitary effect of the inhibitor on ovulation was considered negligible because immature rats were used, and stimulated with exogenous gonadotropins.

XAV939 (catalog item 284028-89-3; Sigma Aldrich, St. Louis, MO, USA) or ICG-001 (catalog item 5.04712.0001; Calbiochem- EMD Millipore, Temecula, CA, USA), dissolved in 20% dimethylsulfoxide, was injected under the bursa of both ovaries (treated groups);

20% dimethylsulfoxide alone was injected into control animals. Doses of 1 µg, 5 µg, or 10 µg of XAV939 or 5 µg o 10 µg of ICG-001 per 5 µl per ovary were tested; 5 µg of XAV939 was later chosen as the standard dose because 1 µg did not change β catenin or circulating progesterone abundance, while 10 µg showed no difference to 5 µg administration.

The treatment with eCG plus hCG causes a considerable (tenfold) increase in ovarian weight due to the stimulation and subsequent transformation of ovarian follicles into corpora lutea. Twenty-four or forty-eight hours after inhibitor administration, animals were euthanized by decapitation without anesthesia. Blood was collected and allowed to clot. Steroids were extracted with ethyl ether, and progesterone was measured by radioimmunoassay. The ovaries were also collected to perform further experiments.

All experimental protocols were approved by the Animal Experimentation Committee of the Instituto de Biología y Medicina Experimental (IByME, Buenos Aires, Argentina) (PHS-NIH Approval Statement of Compliance # A5072–01).

Radioimmunoassay for progesterone

Serum progesterone was measured as described previously (Irusta, Parborell et al. 2003) using specific antibodies supplied by Dr. G.D. Niswender (Animal Reproduction and Biotechnology Laboratory, Colorado State University, Fort Collins, CO, USA). The intra- and inter-assay variations were 8.0% and 14.2%, respectively. The detection limit of the assay was 25 pg progesterone.

Ovarian morphology

Ovaries were removed and immediately fixed in Bouin's fixative (Rosario, Santa Fe, Argentina) for 12 h, and then embedded in paraffin. Five-micron-thick sections were mounted onto microscope slides, according to the method described by Woodruff et al. (Woodruff, Lyon et al. 1990). Every tenth section (50-µm intervals) was mounted to prevent counting the same structure twice. One set of slides was stained with hematoxylin and eosin to count the number of different stages of follicles per ovarian section, while another set of slides was used for histochemical analysis.

Follicles were classified as primary follicles (presence of one cubic granulosa cell layer), preantral follicles, or antral follicles, according to the presence or absence of an antrum, and corpora lutea. Atretic follicles are characterized by the degeneration and detachment of the granulosa cell layer from the basement membrane, the presence of pyknotic nuclei in this cell type, and oocyte degeneration (Andreu, Parborell et al. 1998). Cysts were considered as large, unruptured follicles containing the oocyte and an attenuated granulosa cell layer surrounded by luteal cells. Follicles, corpora lutea, and cysts were quantified in four ovarian sections from each ovary (eight ovaries per treatment). These data were used to calculate the percentage of each ovarian structure due to differences in the size of the ovaries.

Isolation of Corpora lutea

Corpora lutea were dissected from the ovary under a stereoscopic microscope, as previously described (Hernandez, Peluffo et al. 2009; Accialini, Hernandez et al. 2015). Briefly, healthy corpora lutea from four ovaries per group were isolated, frozen, and used

for biochemical assays. The results obtained from the corpora lutea of each ovary were considered as a single datum.

Western blot

For total protein extracts, corpora lutea were resuspended in 300 µl of lysis buffer (20 mM Tris-HCl, pH 8, 137 mM NaCl, 1% Nonidet P-40, and 10% glycerol), supplemented with protease inhibitors (0.5 mM phenylmethylsulfonyl fluoride [PMSF], 0.025 mM N-CBZ-L-phenylalanine chloromethyl ketone, 0.025 mM N-p-tosyl-lysine chloromethyl ketone, and 0.025 mM L-1-tosylamide-2-phenyl-ethylchloromethyl ketone) and phosphatase inhibitors (25 mM sodium fluoride, 0.2 mM sodium orthovanadate, and 10 mM b-glycerophosphate), and homogenized with an Ultra-Turrax homogenizer (IKA-Werke GmbH & Co., Staufen, Germany). Samples were centrifuged at 10,000 xg at 4˚C for 10 min, and the resulting pellets were discarded.

For nuclear protein extracts, corpora lutea were homogenized in buffer TEDGS 10% (50 mM Tris pH 7.4, 7.5 mM EDTA, 0.5 mM dithiothreitol, 10% glycerol, 0.25 M sucrose, 10 µl/ml PMSF, and 10 µl/ml protease inhibitors), and incubated on ice for 30 minutes. The homogenate was centrifuged at 1024xg at 4˚C for 10 minutes, and the pellet was resuspended in wash buffer (TEDGS 10% + 0.01% Nonidet P-40); this centrifugation was repeated. The pellet obtained was resuspended in nucleus buffer (TEDGS 10% + 0.4 M KCl), and mechanically ruptured, incubated on ice for 30 min, and the homogenate was centrifuged at 13540xg at 4˚C for 20 minutes to obtain the nuclear fraction. The supernatant was diluted using an equal volume of buffer TEDGS 30% (50 mM Tris, pH 7.4, 7.5 mM EDTA, 0.5 mM dithiothreitol, 30% glycerol, 0.25 M sucrose, 10 µl/ml PMSF, and 10 µl/ml protease inhibitors).

Protein concentration was measured by the Bradford assay. Twenty micrograms of protein were boiled for 5 min, and then electrophoresed through a 12-15% gradient SDS-polyacrylamide gel at 25 mA for 1.5 h. The resolved proteins were transferred onto nitrocellulose membranes for 2 h. The blot was preincubated for 1 h at room temperature in blocking buffer (5% non-fat milk, 0.05% Tween-20, in Tris-buffered saline [TBS] [137 mM NaCl, 20 mM Tris, pH 7.4]), and then incubated overnight at 4˚C with appropriate primary antibodies (Table 2) diluted in TBS containing 0.1% Tween-20. The blots were then incubated with corresponding secondary antibodies conjugated to horseradish peroxidase (Table 2), and finally detected by chemiluminescence and autoradiography using x-ray film. Protein loading was normalized by reprobing the same blots with antibody against β-actin or Glyceraldehyde 3-phosphate dehydrogenase (GAPDH) (Table 2). Protein abundance was quantified by densitometric analysis using Scion Image Software for Windows (Scion Corporation, Worman's Mill, CT, USA).

Histochemistry

Ovaries were deparaffinized in xylene, and rehydrated by graded ethanol washes. Endogenous peroxidase activity was blocked with hydrogen peroxide in phosphate-buffered saline (PBS), and non-specific binding was blocked for 20 min at room temperature with 2% bovine serum albumin. Sections were incubated overnight at 4˚C with 20 µg/ml biotinylated lectin from *Bandeiraea simplicifolia-1* (Catalog item L3759; Sigma-Aldrich). After washing, the slides were incubated for 30 min at room temperature with horseradish peroxidase-conjugated avidin complex provided in the Vectastain ABC system (Vector Laboratories, Burlingame, CA, USA). Horseradish peroxidase localization was

visualized with diaminobenzidine. The reaction was stopped with distilled water, counterstained with hematoxylin, and dehydrated before mounting with Canada Balsam Synthetic mounting medium (Biopack, Santa Barbara, CA, USA). Negative controls were obtained in the absence of lectin. Digital images were acquired using a camera (Nikon Corporation, Melville, NY, USA) mounted on a conventional light microscope (Nikon).

Images were converted to TIFF format (bilevel scale) for analysis. The endothelial cell area was quantified using ImageJ software (National Institutes of Health, Bethesda, MD, USA) (Rasband 2007). Four sections from each ovary were analyzed (four ovaries per treatment). Only the endothelial cell area in corpora lutea was quantified.

Data analysis

Statistical analysis was carried out using Prism software (version 4.00 for Windows, GraphPad Software, San Diego, California, USA). All experiments were performed at least three times, and each assay was performed in quadruplicate. Four animals per group were used in each experiment. Experiments were analyzed by unpaired Student's *t*-test. Data were expressed as means ± standard errors of pooled results obtained from different independent experiments. Representative gels are shown in the figures. Values of $P<0.05$ were considered significant.

References

Abedini, A., G. Zamberlam, D. Boerboom and C. A. Price (2015). "Non-canonical WNT5A is a potential regulator of granulosa cell function in cattle." Mol Cell Endocrinol **403**: 39-45.

Abramovich, D., G. Irusta, D. Bas, N. I. Cataldi, F. Parborell and M. Tesone (2012). "Angiopoietins/TIE2 System and VEGF Are Involved in Ovarian Function in a DHEA Rat Model of Polycystic Ovary Syndrome." Endocrinology **153**(7): 3446-3456.

Abramovich, D., F. Parborell and M. Tesone (2006). "Effect of a vascular endothelial growth factor (VEGF) inhibitory treatment on the folliculogenesis and ovarian apoptosis in gonadotropin-treated prepubertal rats." Biol.Reprod. **75**(3): 434-441.

Accialini, P., S. F. Hernandez, D. Bas, M. C. Pazos, G. Irusta, D. Abramovich and M. Tesone (2015). "A link between Notch and progesterone maintains the functionality of the rat corpus luteum." Reproduction **149**(1): 1-10.

Andreu, C., F. Parborell, S. Vanzulli, H. Chemes and M. Tesone (1998). "Regulation of follicular luteinization by a gonadotropin-releasing hormone agonist: relationship between steroidogenesis and apoptosis." Mol.Reprod.Dev. **51**(3): 287-294.

Bachelot, A. and N. Binart (2005). "Corpus luteum development: lessons from genetic models in mice." Curr.Top.Dev.Biol **68**: 49-84.

Boyer, A., A. K. Goff and D. Boerboom (2010). "WNT signaling in ovarian follicle biology and tumorigenesis." Trends Endocrinol.Metab **21**(1): 25-32.

Boyer, A., E. Lapointe, X. Zheng, R. G. Cowan, H. Li, S. M. Quirk, F. J. DeMayo, J. S. Richards and D. Boerboom (2010). "WNT4 is required for normal ovarian follicle development and female fertility." FASEB J. **24**(8): 3010-3025.

Carmeliet, P. and R. K. Jain (2011). "Molecular mechanisms and clinical applications of angiogenesis." Nature **473**(7347): 298-307.

Cook, B. D., J. N. Dynek, W. Chang, G. Shostak and S. Smith (2002). "Role for the related poly(ADP-Ribose) polymerases tankyrase 1 and 2 at human telomeres." Mol Cell Biol **22**(1): 332-342.

Christenson, L. K. and R. L. Stouffer (1997). "Follicle-stimulating hormone and luteinizing hormone/chorionic gonadotropin stimulation of vascular endothelial growth factor production by macaque granulosa cells from pre- and periovulatory follicles." J.Clin.Endocrinol.Metab **82**(7): 2135-2142.

Chun, S. Y., H. Billig, J. L. Tilly, I. Furuta, A. Tsafriri and A. J. Hsueh (1994). "Gonadotropin suppression of apoptosis in cultured preovulatory follicles: mediatory role of endogenous insulin-like growth factor I." Endocrinology **135**(5): 1845-1853.

Grigson, E. R., M. Ozerova, A. Pisklakova, H. Liu, D. M. Sullivan and Y. Nefedova (2015). "Canonical Wnt pathway inhibitor ICG-001 induces cytotoxicity of multiple myeloma cells in Wnt-independent manner." PLoS One **10**(1): e0117693.

Guo, X., A. Ramirez, D. S. Waddell, Z. Li, X. Liu and X. F. Wang (2008). "Axin and GSK3- control Smad3 protein stability and modulate TGF- signaling." Genes Dev **22**(1): 106-120.

Gupta, P. S., J. K. Folger, S. K. Rajput, L. Lv, J. Yao, J. J. Ireland and G. W. Smith (2014). "Regulation and regulatory role of WNT signaling in potentiating FSH action during bovine dominant follicle selection." PLoS One **9**(6): e100201.

Hernandez, F., M. C. Peluffo, D. Bas, R. L. Stouffer and M. Tesone (2009). "Local effects of the sphingosine 1-phosphate on prostaglandin F2alpha-induced luteolysis in the pregnant rat." Mol.Reprod.Dev.

Hernandez Gifford, J. A. (2015). "The role of WNT signaling in adult ovarian folliculogenesis." Reproduction **150**(4): R137-R148.

Hsiao, S. J. and S. Smith (2008). "Tankyrase function at telomeres, spindle poles, and beyond." Biochimie **90**(1): 83-92.

Hsieh, M., M. A. Johnson, N. M. Greenberg and J. S. Richards (2002). "Regulated expression of Wnts and Frizzleds at specific stages of follicular development in the rodent ovary." Endocrinology **143**(3): 898-908.

Hsieh, M., S. M. Mulders, R. R. Friis, A. Dharmarajan and J. S. Richards (2003). "Expression and localization of secreted frizzled-related protein-4 in the rodent ovary: evidence for selective up-regulation in luteinized granulosa cells." Endocrinology **144**(10): 4597-4606.

Huang, S. M., Y. M. Mishina, S. Liu, A. Cheung, F. Stegmeier, G. A. Michaud, O. Charlat, E. Wiellette, Y. Zhang, S. Wiessner, M. Hild, X. Shi, C. J. Wilson, C. Mickanin, V. Myer, A. Fazal, R. Tomlinson, F. Serluca, W. Shao, H. Cheng, M. Shultz, C. Rau, M. Schirle, J. Schlegl, S. Ghidelli, S. Fawell, C. Lu, D. Curtis, M. W. Kirschner, C. Lengauer, P. M. Finan, J. A. Tallarico, T. Bouwmeester, J. A. Porter, A. Bauer and F. Cong (2009). "Tankyrase inhibition stabilizes axin and antagonizes Wnt signalling." Nature **461**(7264): 614-620.

Hunzicker-Dunn, M. and E. T. Maizels (2006). "FSH signaling pathways in immature granulosa cells that regulate target gene expression: branching out from protein kinase A." Cell Signal. **18**(9): 1351-1359.

Irusta, G., F. Parborell, M. Peluffo, P. R. Manna, S. I. Gonzalez-Calvar, R. Calandra, D. M. Stocco and M. Tesone (2003). "Steroidogenic acute regulatory protein in ovarian follicles of gonadotropin-stimulated rats is regulated by a gonadotropin-releasing hormone agonist." Biol.Reprod. **68**(5): 1577-1583.

Kaminker, P. G., S. H. Kim, R. D. Taylor, Y. Zebarjadian, W. D. Funk, G. B. Morin, P. Yaswen and J. Campisi (2001). "TANK2, a new TRF1-associated poly(ADP-ribose) polymerase, causes rapid induction of cell death upon overexpression." J Biol Chem **276**(38): 35891-35899.

Korsmeyer, S. J. (1992). "Bcl-2 initiates a new category of oncogenes: regulators of cell death." Blood **80**(4): 879-886.

Li, Q., S. Lin, X. Wang, G. Lian, Z. Lu, H. Guo, K. Ruan, Y. Wang, Z. Ye, J. Han and S. C. Lin (2009). "Axin determines cell fate by controlling the p53 activation threshold after DNA damage." Nat Cell Biol **11**(9): 1128-1134.

Lieberman, S., N. J. Greenfield and A. Wolfson (1984). "A heuristic proposal for understanding steroidogenic processes." Endocr.Rev. **5**(1): 128-148.

Liu, W., H. Rui, J. Wang, S. Lin, Y. He, M. Chen, Q. Li, Z. Ye, S. Zhang, S. C. Chan, Y. G. Chen, J. Han and S. C. Lin (2006). "Axin is a scaffold protein in TGF-beta signaling that promotes degradation of Smad7 by Arkadia." EMBO J **25**(8): 1646-1658.

Logan, C. Y. and R. Nusse (2004). "The Wnt signaling pathway in development and disease." Annu.Rev.Cell Dev.Biol. **20**: 781-810.

Lyons, R. J., R. Deane, D. K. Lynch, Z. S. Ye, G. M. Sanderson, H. J. Eyre, G. R. Sutherland and R. J. Daly (2001). "Identification of a novel human tankyrase through its interaction with the adaptor protein Grb14." J Biol Chem **276**(20): 17172-17180.

Maes, C., P. Carmeliet, K. Moermans, I. Stockmans, N. Smets, D. Collen, R. Bouillon and G. Carmeliet (2002). "Impaired angiogenesis and endochondral bone formation in mice lacking the vascular endothelial growth factor isoforms VEGF164 and VEGF188." Mech.Dev. **111**(1-2): 61-73.

Maga, G. and U. Hubscher (2003). "Proliferating cell nuclear antigen (PCNA): a dancer with many partners." J.Cell Sci. **116**(Pt 15): 3051-3060.

Maisonpierre, P. C., C. Suri, P. F. Jones, S. Bartunkova, S. J. Wiegand, C. Radziejewski, D. Compton, J. McClain, T. H. Aldrich, N. Papadopoulos, T. J. Daly, S. Davis, T. N. Sato and G. D. Yancopoulos (1997). "Angiopoietin-2, a natural antagonist for Tie2 that disrupts in vivo angiogenesis." Science **277**(5322): 55-60.

Martinez-Chequer, J. C., R. L. Stouffer, T. M. Hazzard, P. E. Patton and T. A. Molskness (2003). "Insulin-like growth factors-1 and -2, but not hypoxia, synergize with gonadotropin hormone to promote vascular endothelial growth factor-A secretion by monkey granulosa cells from preovulatory follicles." Biol.Reprod. **68**(4): 1112-1118.

Pascuali, N., L. Scotti, D. Abramovich, G. Irusta, M. Di Pietro, D. Bas, M. Tesone and F. Parborell (2015). "Inhibition of platelet-derived growth factor (PDGF) receptor affects follicular development and ovarian proliferation, apoptosis and angiogenesis in prepubertal eCG-treated rats." Mol Cell Endocrinol **412**: 148-158.

Peluso, J. J., A. M. Luciano, A. Pappalardo and B. A. White (1995). "Cellular and molecular mechanisms that mediate insulin-dependent rat granulosa cell mitosis." Biol.Reprod. **52**(1): 124-130.

Peng, L., J. Arensburg, J. Orly and A. H. Payne (2002). "The murine 3beta-hydroxysteroid dehydrogenase (3beta-HSD) gene family: a postulated role for 3beta-HSD VI during early pregnancy." Mol.Cell Endocrinol. **187**(1-2): 213-221.

Rasband, W. S. (2007). "ImageJ, U. S." National Institutes of Health, Bethesda, Maryland, USA, http://rsb.info.nih.gov/ij/, 1997-.

Redmer, D. A. and L. P. Reynolds (1996). "Angiogenesis in the ovary." Rev.Reprod. **1**(3): 182-192.

Reis, M. and S. Liebner (2013). "Wnt signaling in the vasculature." Exp.Cell Res. **319**(9): 1317-1323.

Roy, L., C. A. McDonald, C. Jiang, D. Maroni, A. J. Zeleznik, T. A. Wyatt, X. Hou and J. S. Davis (2009). "Convergence of 3',5'-cyclic adenosine 5'-monophosphate/protein kinase A and glycogen synthase kinase-3beta/beta-catenin signaling in corpus luteum progesterone synthesis." Endocrinology **150**(11): 5036-5045.

Scotti, L., F. Parborell, G. Irusta, Z. de, I, C. Bisioli, H. Pettorossi, M. Tesone and D. Abramovich (2014). "Platelet-derived growth factor BB and DD and angiopoietin1 are altered in follicular fluid from polycystic ovary syndrome patients." Mol.Reprod.Dev. **81**(8): 748-756.

Smith, S., I. Giriat, A. Schmitt and T. de Lange (1998). "Tankyrase, a poly(ADP-ribose) polymerase at human telomeres." Science **282**(5393): 1484-1487.

Stocco, C., C. Telleria and G. Gibori (2007). "The molecular control of corpus luteum formation, function, and regression." Endocr.Rev. **28**(1): 117-149.

Stocco, D. M. and B. J. Clark (1996). "Regulation of the acute production of steroids in steroidogenic cells." Endocr.Rev. **17**(3): 221-244.

Suri, C., P. F. Jones, S. Patan, S. Bartunkova, P. C. Maisonpierre, S. Davis, T. N. Sato and G. D. Yancopoulos (1996). "Requisite role of angiopoietin-1, a ligand for the TIE2 receptor, during embryonic angiogenesis." Cell **87**(7): 1171-1180.

Tamanini, C. and M. De Ambrogi (2004). "Angiogenesis in developing follicle and corpus luteum." Reprod.Domest.Anim **39**(4): 206-216.

Tesone, M., R. L. Stouffer, S. M. Borman, J. D. Hennebold and T. A. Molskness (2005). "Vascular endothelial growth factor (VEGF) production by the monkey corpus luteum during the menstrual cycle: isoform-selective messenger RNA expression in vivo and hypoxia-regulated protein secretion in vitro." Biol Reprod. **73**(5): 927-934.

Tilly, J. L. and K. I. Tilly (1995). "Inhibitors of oxidative stress mimic the ability of follicle-stimulating hormone to suppress apoptosis in cultured rat ovarian follicles." Endocrinology **136**(1): 242-252.

Tomizuka, K., K. Horikoshi, R. Kitada, Y. Sugawara, Y. Iba, A. Kojima, A. Yoshitome, K. Yamawaki, M. Amagai, A. Inoue, T. Oshima and M. Kakitani (2008). "R-spondin1 plays an essential role in ovarian development through positively regulating Wnt-4 signaling." Hum.Mol.Genet. **17**(9): 1278-1291.

Vainio, S., M. Heikkila, A. Kispert, N. Chin and A. P. McMahon (1999). "Female development in mammals is regulated by Wnt-4 signalling." Nature **397**(6718): 405-409.

Waterman, M. R. and E. R. Simpson (1985). "Regulation of the biosynthesis of cytochromes P-450 involved in steroid hormone synthesis." Mol.Cell Endocrinol. **39**(2): 81-89.

Woodruff, T. K., R. J. Lyon, S. E. Hansen, G. C. Rice and J. P. Mather (1990). "Inhibin and activin locally regulate rat ovarian folliculogenesis." Endocrinology **127**(6): 3196-3205.

Figures legends

Figure 1. Effect of 5 µg XAV939 administration on β-catenin content, 24h and 48 hours after inhibitor treatment. Optical density is expressed in arbitrary units ± standard error, normalized to β-actin. Representative immunoblots of protein content are shown in the lower panel. *, $P<0.05$ for control (n=6) versus XAV939 (n=8) groups.

Figure 2. Histological effects of β-catenin signaling inhibition on ovaries. Representative sections from (a) control and XAV939-treated or (b) control and ICG-001-treated ovaries. Scale bars, 200 µm. AF, antral follicle; CL, corpus luteum; Cyst, cystic structures.

Figure 3. Effect of 5 µg XAV939 administration on progesterone production and steroidogenic regulators. (a) Serum progesterone levels 48 hours after XAV939 treatment, measured by radioimmunoassay. *, $P<0.05$ (n=8). (b-d) Western blot quantification of corpus luteum protein abundance of (b) StAR, (c) cytochrome P450scc, and (d) 3β-HSD 48 hours after XAV939 treatment. Optical density is expressed in arbitrary units ± standard error, normalized to Glyceraldehyde 3-phosphate dehydrogenase (GAPDH). Representative immunoblots of protein content are shown in the lower panel. *, $P<0.05$ for control (n=6) versus XAV939 (n=8) groups.

Figure 4. Effect of XAV939 on proliferation corpus luteal cells. (a) Western blot quantification of PCNA abundance 48 hours after XAV939 treatment in corpora lutea. Optical density is expressed as arbitrary units ± standard error, normalized to Glyceraldehyde 3-phosphate dehydrogenase (GAPDH). Representative immunoblots of

protein content are shown in the lower panel. *, $P<0.05$ for control (n=6) versus XAV939 (n=8) groups. (b) Representative PCNA immunohistochemistry in an ovary section from the control group. Inset shows the negative-control staining. Arrows indicate staining of PCNA protein in small cells. Scale bar, 50 μm.

Figure 5. Effect of XAV939 administration on pro- and anti-apoptotic protein content. (a-c) Western blot quantification of corpus luteum protein abundance of pro-apoptotic proteins (a) $BCLX_S$ and (b) BAX or anti-apoptotic (c) $BCLX_L$, 48 hours after XAV939 treatment. Optical density is expressed as arbitrary units ± standard error, normalized to β-actin. Representative immunoblots of protein content are shown in the lower panel. (d-e) Luteal $BCLX_S/BCLX_L$ (d) and $BAX/BCLX_L$ (e) ratio. *, $P<0.05$ for control (n=6) versus XAV939 (n=8) groups.

Figure 6. Effect of XAV939 administration on ERK and AKT pathway in corpora lutea. Western blot quantification of (a) ERK and (b) AKT phosphorylation 24 hours after XAV939 treatment. The ratio between phosphorylated and total proteins are expressed as arbitrary units ± standard error. Representative immunoblots of protein content are shown in the lower panel. *, $P<0.05$ for control (n=5) versus XAV939 (n=4) groups.

Figure 7. Effect of XAV939 administration on angiogenic factors. Western blot quantification of corpora lutea (a) VEGF164 and (b) VEGF120 abundance 24 hours after XAV939 treatment. Optical density is expressed as arbitrary units ± standard error, normalized to Glyceraldehyde 3-phosphate dehydrogenase (GAPDH). Representative immunoblots of protein content are shown in the lower panel. *, $P<0.05$ (n=4 per group).

Figure 8. Effect of XAV939 administration on vascular development. (a) Quantification of endothelial cell area in corpora lutea of treated and control ovarian sections. *, $P<0.05$ (n=4 per group). (b) Histological sections of control and XAV939-treated ovaries stained with *Bandeiraea simplicifolia* 1 lectin. Insets show a higher magnification of a corpus luteum. Scale bars, 200 μm (panels) or 50 μm (insets).

Figure 9. Role of Wnt/β-catenin pathway on rat corpus luteum development.

Tankyrases (TNK) are enzymes that PARsylate (add poly-ADP-ribose) different substrates, promoting their degradation. TNKs PARsylate Axin, a protein that promotes the ubiquitination and proteasomal degradation of β-catenin. Activation of the canonical Wnt pathway retains high levels of β-catenin, allowing it to translocate to the nucleus, where it regulates the transcription of target genes. XAV939 is a small molecule that inhibits TNK. Administration of XAV939 leads to phosphorylation and degradation of β-catenin, and subsequent inhibition of target gene expression (e.g. the *Star* gene). This leads to a decrease in progesterone levels, which may affect the corpora lutea survival, given that this hormone plays a protective role against apoptosis in the rodent corpus luteum (Stocco et al., 2007). Loss of β-catenin signaling also reduces ERK signaling, decreases VEGF-A abundance, and subsequently decreases cell proliferation. These ultimately result in a reduction in endothelial cell area, reflecting impaired corpus luteal vascular development.

Table 1. Antibodies used for immunohistochemistry and western blot.

Peptide target	Manufacturer, catalog number†	Species raised in	Dilution
β-ACTIN	Cell Signaling, #4967	Rabbit	1:10,000
AKT	Cell Signaling, #9272	Rabbit	1:8000
phospho-AKT	Santa Cruz Biotechnology, #sc-7985-R	Rabbit	1:1000
BAX	Santa Cruz Biotechnology, #sc-493	Rabbit	1:750
BCLX	Santa Cruz Biotechnology, #sc-634	Rabbit	1:200
β-CATENIN	Santa Cruz Biotechnology, #sc-59737 (12F7)	Mouse	1:1000
ERK	Santa Cruz Biotechnology, #sc-154	Rabbit	1:2000
phospho-ERK	Santa Cruz Biotechnology, #sc-7383	Mouse	1:1000
GAPDH	Cell Signaling, # 2118	Rabbit	1:10000
3β-HSD	Santa Cruz Biotechnology, #sc-30820 (P-18)	Goat	1:200
P450scc	Dr. Anita Payne. Stanford University Medical Center, Stanford, CA, USA	Rabbit	1:200
StAR	Santa Cruz Biotechnology,	Rabbit	1:200

	#sc-25806		
VEGF *	Abcam, #ab46154	Rabbit	1:1000
Anti-rabbit horseradish peroxidase IgG	Sigma-Aldrich #A-4914		1:1000
Anti-mouse horseradish peroxidase IgG	R&D Systems, #HAF007		1:1000
Anti-goat horseradish peroxidase IgG	Bio Rad, #772-1034		1:1000
Biotinylated anti-rabbit IgG	Vector Laboratories, Vectastain ABC system		1:400

* Recognizes VEGF 164 and 120 isoforms

† Abcam (Cambridge, MA, USA); BioRad Laboratories (Hercules, CA, USA); Cell Signaling (Danvers, MA, USA); R&D Systems (Minneapolis, MN, USA); Santa Cruz Biotechnology, Inc. (Santa Cruz, CA, USA); Sigma-Aldrich (St Louis, MO, USA); Vector Laboratories, Burlingame, CA, USA

Structure	**Control** (n=10)	**XAV939** (n=10)
Primary	4.9 ± 1.2	6.3 ± 1.2
Preantral	6.3 ± 0.9	10.5 ± 2.4
Antral	34.5 ± 3.8	32.3± 5.6
Atretic	9.6 ± 2.9	10.1 ± 2.8
Corpus lutea	45.8 ± 5.0	30.9 ± 4.0*
Cyst	1.0 ± 0.8	8.7 ± 1.0**

Table 2. Follicular and luteal development in control and XAV939-treated rats.

The percentage (mean ± standard error) of each structure in ovarian sections, stained with hematoxylin and eosin, is displayed. *, $p<0.05$; **, $p<0.001$ compared to control ovaries.

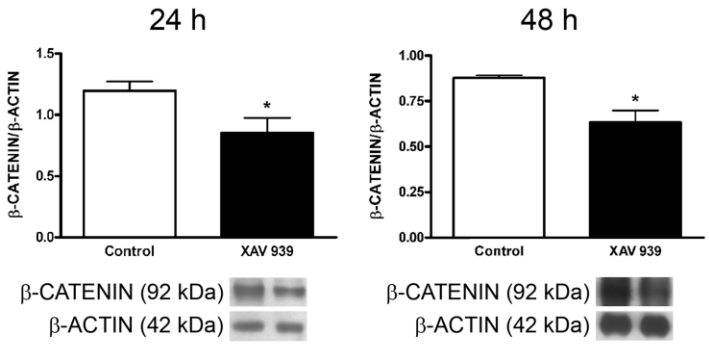

Figure 1

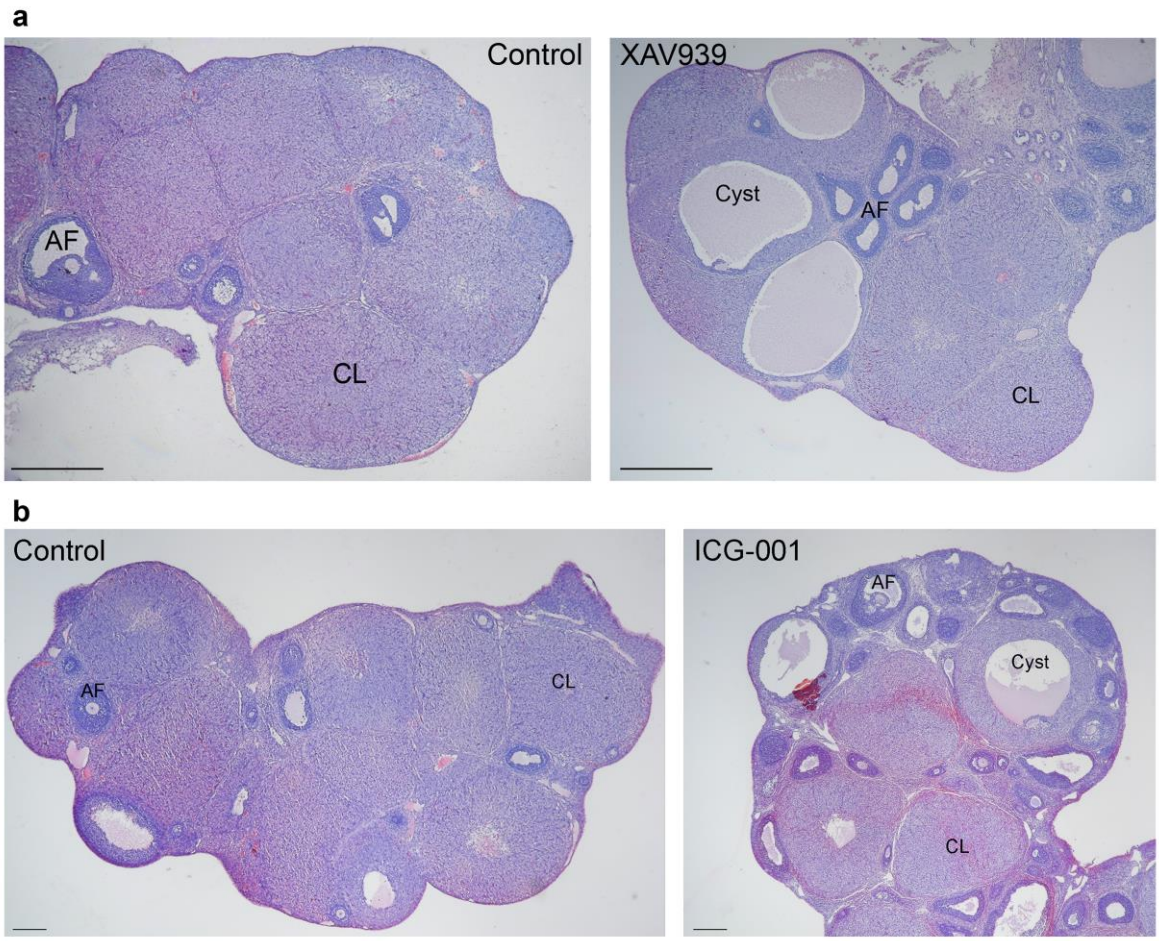

Figure 2

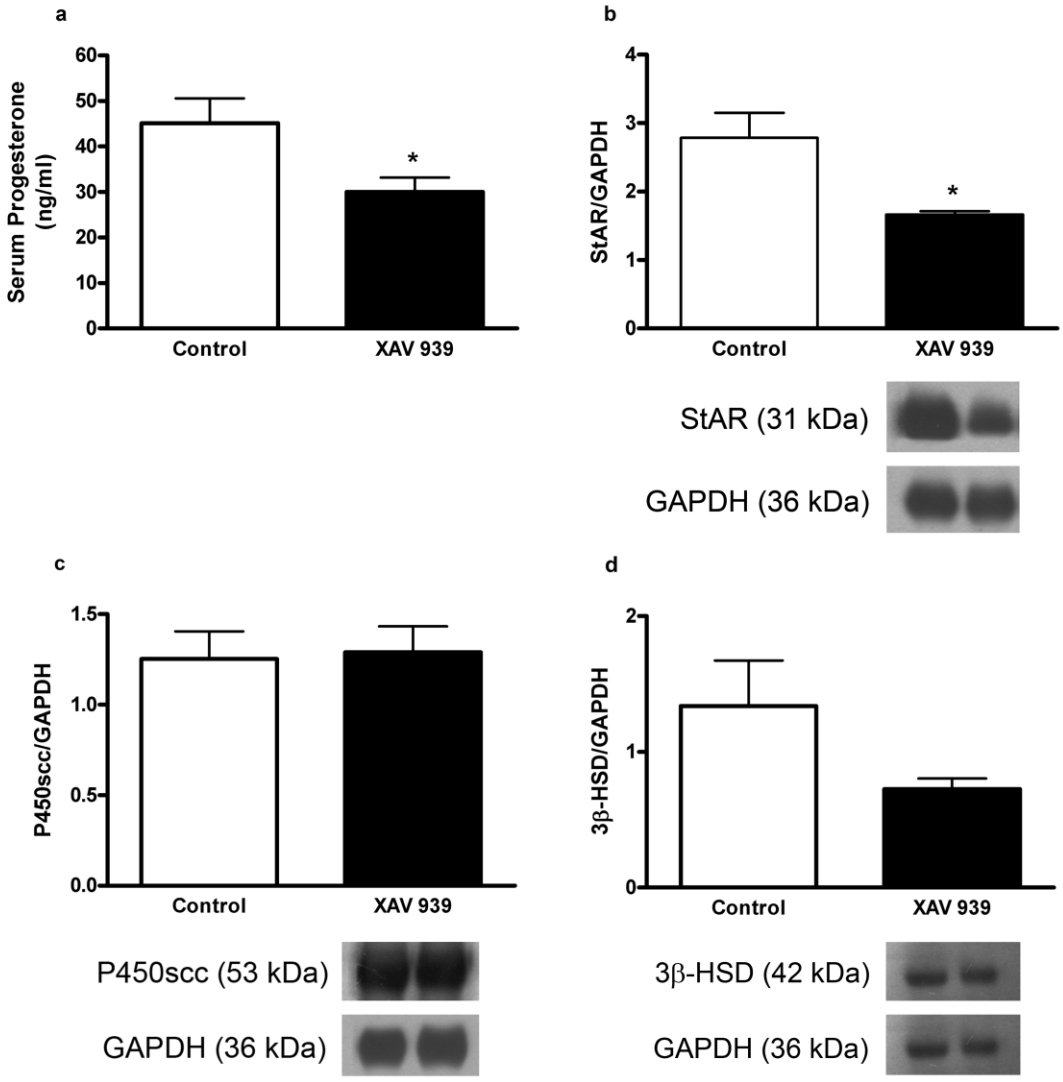

Figure 3

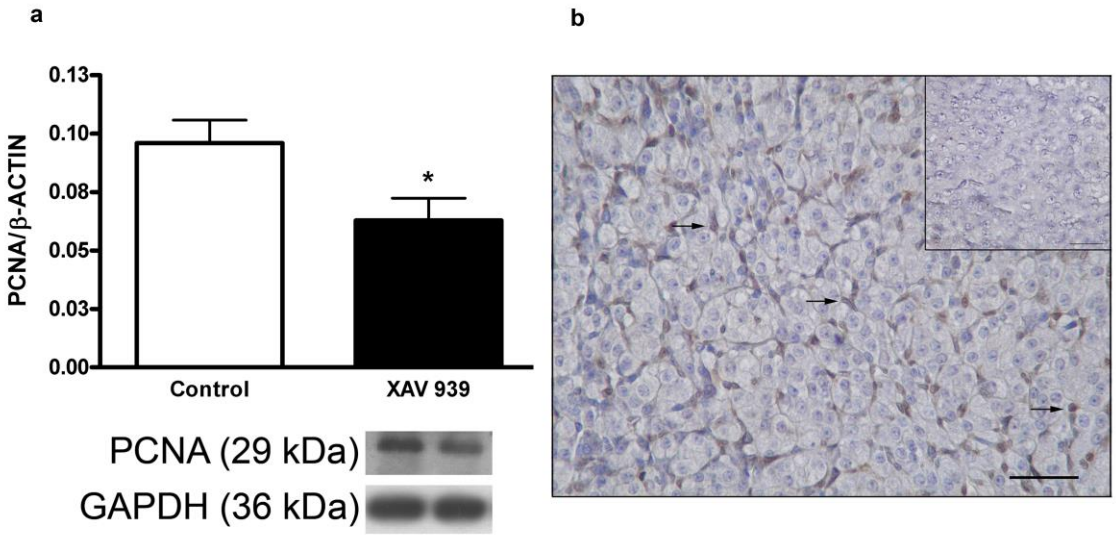

Figure 4

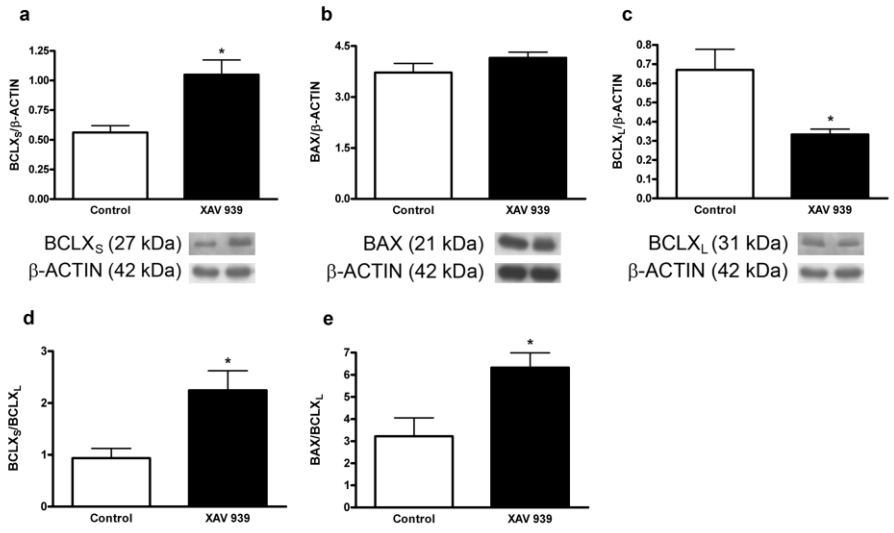

Figure 5

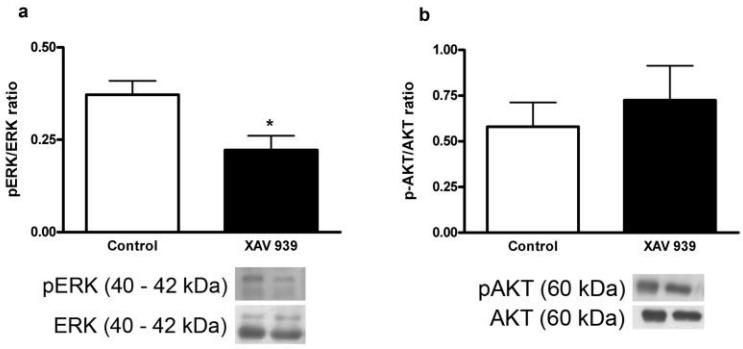

Figure 6

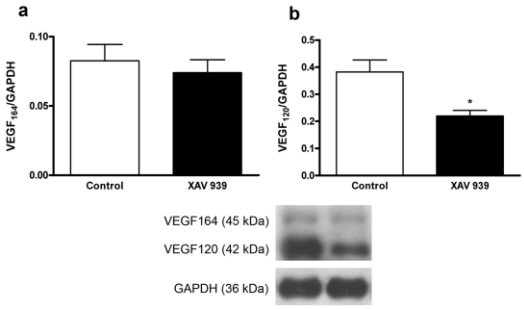

Figure 7

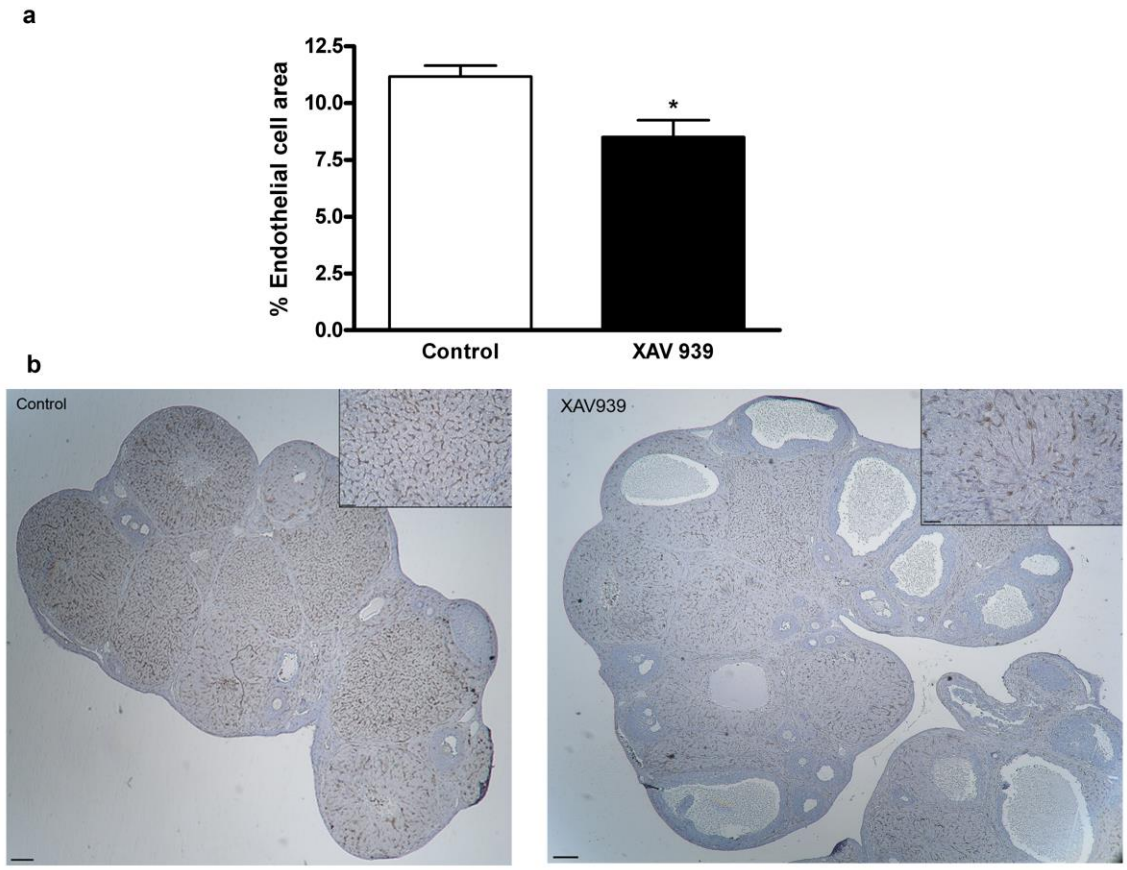

Figure 8

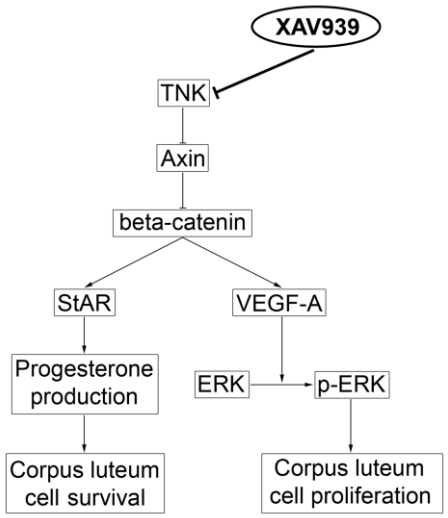

Figure 9